NASA TM X-508

22 p.

TECHNICAL MEMORANDUM

X-508

MEASUREMENTS OF THERMAL RADIATION OF AIR FROM THE STAGNATION REGION OF BLUNT BODIES TRAVELING AT VELOCITIES UP TO 31,000 FEET PER SECOND

By William A. Page, Thomas N. Canning, Roger A. Craig, and Jack D. Stephenson

Ames Research Center
Moffett Field, Calif.

NATIONAL AERONAUTICS AND SPACE ADMINISTRATION

WASHINGTON

June 1961

NATIONAL AERONAUTICS AND SPACE ADMINISTRATION

TECHNICAL MEMORANDUM X-508

MEASUREMENTS OF THERMAL RADIATION OF AIR FROM THE STAGNATION REGION OF BLUNT BODIES TRAVELING AT VELOCITIES UP TO 31,000 FEET PER SECOND*

By William A. Page, Thomas N. Canning, Roger A. Craig, and Jack D. Stephenson

SUMMARY

Preliminary measurements are reported of the total intensity of thermal radiation from the gas cap (i.e., region between shock and body in vicinity of stagnation point) of blunt bodies traveling at velocities from 10,000 to 31,000 feet per second. In general, at the higher free-stream densities, where equilibrium radiation is expected, the results obtained agree reasonably well with the available equilibrium radiation theories. At the lower densities, however, as much as 30 times the theoretical equilibrium radiation is observed, apparently caused by failure of the gas in the shock layer to reach thermodynamic and chemical equilibrium. The altitude for the onset of nonequilibrium radiation for velocities above 20,000 feet per second is found to occur at about 33 miles for a body with a nose radius of 1 foot.

INTRODUCTION

The aerodynamic heating of space vehicles during entry into the earth's atmosphere has become an immediate problem of practical concern. At circular entry velocity, convection is responsible for the important heat load; but, as velocities increase to parabolic or higher, an additional form of heating - thermal radiation from the hot gases in the layer between the bow shock and body surface - is expected to be of equal or of greater importance. To design safe, efficient heat shields for vehicles entering at these high velocities, it will be necessary to study the characteristics and severity of radiation heating. Not only will total radiation intensities of the hot gases have to be determined, but it will be necessary to measure the spectral distribution of the radiation, to determine what fraction of the radiated energy is absorbed by the body

*Title, Unclassified

surface, and to determine how this energy influences the properties of heat-shield materials.

Ames Research Center has embarked upon a research program to study various aspects of this problem. The present report presents preliminary experimental information obtained to date on the total intensity of the radiation emitted by the hot-gas cap of blunt bodies traveling at velocities from 10,000 to 31,000 feet per second. The results are compared with available theories.

SYMBOLS

e	voltage output of radiation detector
E_t	total radiation per unit volume, watts/cm^3
E_{t_λ}	total radiation per unit volume per unit wavelength, watts/cm^3 micron
F	fraction of total spectral radiation responded to by radiation detector
I	radiation intensity, watts
I_λ	radiation intensity per unit wavelength, watts/micron
K	radiation detector calibration constant, volts/watt
L_λ	intensity per unit wavelength of tungsten calibrating lamp, watts/micron
M	Mach number
R_λ	relative spectral response of radiation detector as function of wavelength, ($R_{\lambda_{max}} = 1.0$)
T	temperature in gas cap, computed for equilibrium conditions behind normal shock wave, $^\circ$K
V_∞	total velocity, ft/sec
λ	wavelength, microns
ρ	density in gas cap, computed for equilibrium conditions behind normal shock wave

A 5 0 7

ρ_o sea-level density at 273° K

ρ_∞ free-stream density

APPARATUS AND INSTRUMENTATION

To obtain the high velocities required for a study of thermal radiation from hot-gas layers a pilot hypersonic free-flight facility, depicted in figure 1, was constructed. The facility consists of a light-gas gun which launches models into either still air or into an advancing air stream generated in the test section of a shock-tube-driven supersonic wind tunnel. The velocities obtainable from the light-gas gun range from 10,000 to 25,500 feet per second. The nominal stream velocity and Mach number in the test section are 6,000 feet per second and 6, respectively. To simulate flight at various altitudes in the atmosphere, the pressure level in the shock tube and hence the free-stream pressure in the test section can be controlled. For the present tests, the range of free-stream pressures extended from 0.03 to 1.75 psia.

Instrumentation installed in the measuring section of the test region consists of: (a) two spark shadowgraph stations which are used in conjunction with electronic-counter chronographs to determine the velocity of the model (A typical shadowgraph is shown in figure 2.); (b) pressure pickup in the wall of the wind-tunnel test section to determine time history of the static pressure of the flow in the test section; (c) pressure pickup in the wall at the nozzle end of the pump tube to determine time history of stagnation pressure driving the Mach number 6 nozzle. A typical record of the stagnation and static pressures is shown in figure 3.

The following method was utilized to compute stream properties, in particular, density and velocity. The pressure record obtained in the shock tube of the reflected shock strength allows the computation of stagnation temperature from the real-gas charts of reference 1. A Mollier chart for air determines the stagnation enthalpy. The expansion of the flow through the wind-tunnel nozzle to stream conditions in the test section is assumed to proceed at constant entropy. The stream Mach number was measured utilizing shadowgraphs of the flow about a stationary cone installed in the test section. From the stagnation enthalpy and Mach number the remaining properties of the stream are computed; density, pressure, temperature, and velocity. The stream pressure so computed was found to agree with measured values for the several cases that were checked to within 3 percent. Computed stream velocities ranged from 5,000 to 5,850 feet per second, depending upon shock tube loading conditions. The measured stream Mach numbers varied from 5.25 to 5.50.

The models launched by the gun were spherical nosed polyethylene or polycarbonate plastic cylinders, 0.28 inch in diameter, with nose radius of 0.20 inch. The half angle subtended by the model face at the radius of curvature was 44.4°.

Radiation data were obtained with either RCA 1P21 or RCA 1P28 photomultiplier tubes, which viewed the model at right angles to the flight path. The experimental setup is depicted in figure 4, along with a typical oscilloscope trace of the phototube output. The pair of slits, one-half by one inch in size, were used to allow measurement of the intensity of the gas-cap radiation with a minimum of interference from radiation originating in the model wake.

REDUCTION OF RADIATION DATA

Calibration of the photomultiplier tubes to determine their sensitivities to incident radiation was made with a tungsten lamp calibrated by the National Bureau of Standards. When the phototube views the standard lamp under geometric conditions identical to those used in the test setup (i.e., at the same distance and mounted in the same slit assembly), its voltage output is given by

$$e = K \int_0^\infty R_\lambda L_\lambda d\lambda \qquad (1)$$

where R_λ is the relative spectral response of the phototube as a function of wavelength, L_λ is the spectral output of the standard lamp in watts per micron, and K is the phototube calibration constant in volts per watt of radiant energy. The relative spectral response functions, R_λ, for the particular photomultiplier tubes used are presented in figure 5. Since the functions in the integrand of equation (1) are known, the integral may be evaluated. When the phototube is exposed to the standard lamp at the specified distance, a measurement of its output voltage, e, will define the constant K. Similarly, when the phototube views the radiation from the model gas cap, its output is given by

$$e = K \int_0^\infty R_\lambda I_\lambda d\lambda \qquad (2)$$

where now I_λ is the spectral output of the radiation from the gas cap in watts per micron. In the present instance, the quantity desired is the total radiation from the gas cap, or

$$I = \int_0^\infty I_\lambda d\lambda \qquad (3)$$

This quantity cannot be determined without prior information, at the very least, of the relative shape of the spectral distribution, I_λ, of the radiation from the gas cap. In another sense, because of its limited spectral response, R_λ, the phototube responds to only a fraction of the total radiation from the gas cap. This fraction, F, given by

$$F = \frac{\int_0^\infty R_\lambda I_\lambda d\lambda}{\int_0^\infty I_\lambda d\lambda} \tag{4}$$

was estimated by utilizing the theoretical spectral distributions of equilibrium radiation from high-temperature air presented in reference 2. By combining equations (2), (3), and (4), the total radiation from the gas cap is given by

$$I = \frac{1}{F}\frac{e}{K} \tag{5}$$

To report the results of the present tests in terms of the total radiation per unit volume of the hot gases, the effective radiating volume of the gas cap, assumed to be emitting the radiation at constant conditions, was estimated utilizing the following procedure: (a) The bow shock standoff distance for the stagnation point streamline was determined by use of the theory of reference 3. (b) The standoff distance of the bow shock was considered to be uniform over the spherical face of the model. (c) The distribution of radiation intensity, directly behind the bow shock along its length and along the model surface from the stagnation point to the model shoulder (assumed for simplicity to be the sonic point of the flow), was estimated by computing the temperature and density, and then the equilibrium radiation from the theory of reference 2. From these computations, it was found that the effective radiating volume, assuming all the gas to be at the conditions existing directly behind the normal bow shock, could be approximated by one-half the total volume of the gas cap. The foregoing procedure for determining the effective radiating volume of the gas cap has several recognized weaknesses not the least of which are (a) the utilization of a theory for the standoff distance not yet confirmed by experimental evidence for the high velocities of the experimental data reported herein, and (b) the use of the assumption that the shock standoff distance is uniform when there is available evidence that, for a spherical nose, it increases somewhat with distance from the stagnation point. It is believed, however, from consideration of the computations mentioned above that the effective radiating volume has been determined to 30-percent accuracy. The computational labor involved in obtaining a more accurate estimate which would include a point-by-point analysis of the flow field is not considered justified at the present time because of the random scatter in the radiation data presented later.

Two other minor effects were considered in the reduction of the radiation data; however, they tended to cancel each other. It was estimated that the radiation from that part of the gas cap hidden from view behind the bulge of the model face was compensated for by the radiation reflected back toward the phototube from the model face that was in view.

AVAILABLE THEORIES

The general theory of the emission of radiation by atoms and molecules has long been under intensive study and is the subject matter of many publications. With the additional availability of information on the constituents of high-temperature air under equilibrium conditions - and some experimental measurements to help in the determination of oscillator strengths - several papers, which are in reasonable agreement, have been published, giving estimates of the equilibrium radiation characteristics of air at high temperatures and at various densities. The predictions for the total radiation given in references 2 and 4 are shown in figure 6 over the density range of interest herein. Results labeled reference 2 were obtained by appropriate integration of the absorption coefficients presented in the reference. In addition to the above information, figure 7 shows the predictions of spectral distributions from reference 2 for several selected densities and equilibrium temperatures. The figure shows that, in general, most of the radiation energy is concentrated in the ultraviolet range. It should be mentioned that it was these theoretical spectral distributions which were used to determine the estimated fraction of the spectral radiation seen by the radiation pickups as discussed in the previous section.

RESULTS AND DISCUSSION

The experimental data obtained to date on radiation intensity from hot-gas caps of blunt bodies traveling at hypersonic velocities are summarized in table I. Included in the table are the observed radiation intensities deduced from the measurements made with the photomultipliers and the results of all the computations that allow presentation of the data in a form directly comparable with the predictions of the available theories.

Calculations indicated that the front faces of the plastic models were ablating (model material sublimation due to the high convective heat transfer) when the models passed the radiation detector station. An evaluation of the possibility that the ablation products contributed to the radiation observed indicate that in the worse case, approximately 10 percent of the mass in the gas cap is vaporized material from the model surface. For this material to significantly increase the radiation observed, it would be necessary for the ablation products to be rapidly heated to the order of the temperature of the gas cap. Since the surface temperature of the plastic is less than 1000° K, whereas the gas-cap temperature is near 10,000° K, it appears as likely the vaporized ablation products decrease instead of increase the radiation observed due to a lowering of the average temperature of the gas near the body surface. It

would thus appear that the effects of ablation on the radiation observed for this investigation are probably small, but whether there is an increase or decrease of the radiation is presently unknown.

Figure 8 presents the experimental results in terms of the total radiation per unit volume compared with the equilibrium theories of references 2 and 4. The figure was prepared utilizing the normalizing factor $(\rho/\rho_o)^{1.7}$, chosen so as to collapse the theoretical curves for different densities to a single line as nearly as possible. Shading on the figure represents the remaining variation of the theory over the density range specified. Inspection of the figure shows that a majority of the experimental data agrees favorably with the equilibrium theory even though the normalized total radiation varies over almost five orders of magnitude. An appreciation of the random errors of the experimental information can be obtained from consideration of the scatter of the data near a given velocity and density. A sufficient grouping of data points is available in the velocity range from 15,000 to 18,000 feet per second. The scatter can be seen to be at least a factor of two or three. There are, however, data points that deviate to a much greater degree than the aforementioned amount.

A 5 0 7

The most marked deviation of the data from the equilibrium theory is a striking increase (up to 30 times) in normalized radiation for lower densities in the velocity ranges of 21,000 and 30,000 feet per second. This observed increase is thought to be due to failure of the gas in the hot-gas cap to reach thermodynamic and chemical equilibrium during the short time it takes to travel through the gas cap. Lack of thermodynamic and chemical equilibrium leads to higher than equilibrium temperatures behind the shock, and thus to higher radiation intensities. Similar nonequilibrium effects have also been noted in the shock-tube experiments reviewed in reference 5. Reference 5 also contains predictions of a preliminary nature regarding the onset and intensity of nonequilibrium radiation which depend upon the size and density of the gas layer, and the velocity of the stream.

A comparison of the present experimental results obtained near 21,000 and 30,000 feet per second, with the predictions of the onset and intensity of nonequilibrium radiation obtained from reference 5, is shown in figure 9. The curves from the reference are for velocities of 20,000 and 25,000 feet per second, and were originally given in figures 16 and 17 of reference 5 for a vehicle with a nose radius of 1 meter. To make these predictions comparable with the present results, however, it was necessary to convert them to a 0.2-inch nose radius, the radius of the present models. The conversion is done by changing the density for a predicted nonequilibrium radiation increase by the ratio of the size of the two vehicles - in this case, by a ratio of 200. This scaling is equivalent to assuming that the reaction rates controlling the intensity of the nonequilibrium radiation are directly proportional to gas density.

Inspection of figure 9 indicates that for the few experimental data points obtained to date, and particularly for those at 21,000 feet per second, the present results fall as close as a factor of 3 in density to the predicted curves from reference 5. It should also be noted that the rate at which the radiation rises above the equilibrium line agrees fairly well with the predictions. Considering the large extrapolation of 200 in density that was made for this comparison, the agreement shown is quite gratifying. It thus appears that in the present tests as well as those upon which the predictions of reference 5 were based, the same physical phenomenon is causing the increase of radiation over the equilibrium values.

A further and somewhat different presentation of the properties of nonequilibrium radiation is given in figure 10. Here, on a plot of vehicle velocity versus atmospheric density, or altitude, are given the boundaries for the onset of nonequilibrium radiation as derived both from the curves of reference 5 and from the present data which are shown on the previous figure. The boundary values obtained from figure 9 are considered to be at that point where an extension of the linear portion of the curves (or a line drawn through the data points) intersects the horizontal axis where $E_t/E_{t_{equil\ theory}} = 1$. In addition, a further prediction from reference 6 for a boundary to the region where nonequilibrium effects will become important is reproduced. It should be mentioned that the boundary from reference 6 "gives the altitude at which the relaxation time is approximately equal to the time it takes a gas particle to pass through the shock layer" and should be considered as being only roughly indicative of the region where the nonequilibrium radiation contribution to the total radiation becomes significant. All the information shown on the figure has been adjusted to correspond to a vehicle with a nose radius of 1 foot. The data point in figure 10 near 15,000 feet per second, obtained from the present experiments, has not previously been discussed. Reinspection of figure 8 will show that this point was obtained from the anomalous increase in radiation (relative to the theoretical values) at an approximately constant density as the velocity was reduced from 15,000 feet per second. A further point to be made regarding the behavior of the present data near 15,000 feet per second is that since the higher-than-theoretical radiation values occur at the lower velocities, the nonequilibrium boundary must necessarily be rising to higher altitudes as velocity increases. This fact is indicated in figure 10 by the short line drawn through the data point at 15,000 feet per second.

A study of figure 10 reveals the interesting effect of velocity on the nonequilibrium boundary - as velocity is increased, the boundary first appears to rise to higher altitudes, and then as circular velocity is approached and exceeded, it appears to become constant or decrease slightly. In a recent private communication, Bennett Kivel indicated that because of the preliminary nature of the data upon which the predictions of reference 5 are based, the downward trend of the nonequilibrium

boundary with altitude may not be particularly significant. Even though the results shown in figure 10 must be considered as preliminary in nature, it is felt that the altitude region where nonequilibrium radiation occurs has been fairly well established. This region has important significance from the standpoint of predicting the radiation heat-transfer rates to space vehicles entering the atmosphere, particularly if the trajectories pass near the nonequilibrium boundary.

CONCLUDING REMARKS

Preliminary results are reported on the thermal radiation from the hot-gas caps of blunt bodies traveling at velocities from 10,000 to 31,000 feet per second. Thus far, only total intensities of the radiation have been given, since no details of the spectral distribution have yet been measured. The data have been obtained under a sufficient variety of conditions to exhibit the enormous variation of radiation intensity with velocity and density. In general, at the higher free-stream densities, where equilibrium radiation is expected, the results agree reasonably well with the available equilibrium radiation theories.

For specific flight conditions, however, greatly increased radiation intensities have been observed (more than 30 times the expected equilibrium value), apparently caused by failure of the gas in the shock layer to reach thermodynamic and chemical equilibrium. Increased radiation due to such nonequilibrium effects is a function of the size of the gas cap, as well as the air density and the vehicle velocity; thus, it can be expected to occur at all velocities but at differing altitudes, depending upon the size of the vehicle. The altitude at which nonequilibrium effects first appear to occur rises as the velocity increases above 15,000 feet per second, and then, as circular velocity is approached and exceeded, becomes constant or decreases slightly. Knowledge of the altitude regions where nonequilibrium radiation occurs has important significance from the standpoint of predicting the radiation heat-transfer rates to space vehicles entering the atmosphere, particularly if the trajectories pass near the nonequilibrium boundary.

Ames Research Center
National Aeronautics and Space Administration
Moffett Field, Calif., Mar. 17, 1961

[redacted]

REFERENCES

1. Hansen, C. Frederick, and Heims, Steve P.: A Review of the Thermodynamic, Transport, and Chemical Reaction Rate Properties of High-Temperature Air. NACA TN 4359, 1958.

2. Meyerott, R. E., Sokoloff, J., and Nicholls, R. W.: Absorption Coefficients of Air. LMSD 288052, Lockheed Aircraft Corp., 1959.

3. Li, Ting-Yi, and Geiger, Richard E.: Stagnation Point of a Blunt Body in Hypersonic Flow. Jour. Aero. Sci., vol. 24, no. 1, Jan. 1957.

4. Kivel, B., and Bailey, K.: Tables of Radiation From High Temperature Air. Res. Rep. 21, AVCO Res. Lab., 1957.

5. Camm, J. C., Kivel, B., Taylor, R. L., and Teare, J. D.: Absolute Intensity of Nonequilibrium Radiation in Air and Stagnation Heating at High Altitudes. Res. Rep. 93, AVCO Everett Res. Lab., 1959.

6. Kivel, Bennett: Radiation From Hot Air and Its Effect on Stagnation-Point Heating. Jour. Aero/Space Sci., Feb. 1961.

[redacted]

TABLE I.- REDUCTION OF EXPERIMENTAL DATA

Shot	V_∞, ft/sec	ρ/ρ_o	T, ^oK	Effective gas-cap volume, cm^3	I, watts, observed	F	Et, watts/cm^3	$Et/(\rho/\rho_o)^{1.7}$, watts/cm^3	Notes
1	9,450	0.85	3,210	0.0041	0.00258	0.33	1.91	2.50	1P21 data Al. sphere, 0.28 inch dia.
2	11,700	.92	4,030	.0099	.149	.33	45.6	52.9	1P21 data
3	12,300	.82	4,260	.0095	.120	.32	39.4	55.5	
4	12,650	1.11	4,440	.0096	.669	.31	225	189	
5	13,700	.60	4,710	.0090	.285	.28	113	273	
6	13,800	.67	4,800	.0096	.152	.28	56.2	111	
7	14,030	.77	5,010	.0091	.230	.27	93.3	146	
8	15,150	.68	5,580	.0091	.141	.25	61.8	118	
9	16,100	.69	6,030	.0089	.252	.23	123	231	
10	16,400	.68	6,240	.0088	.224	.24	106	204	
11	16,700	.71	6,300	.0086	.217	.25	101	183	
12	17,500	.72	6,720	.0085	.303	.26	137	240	
13	17,730	.94	6,840	.0085	.450	.26	204	229	
14	17,900	.73	6,720	.0084	.639	.26	292	498	
15*	20,500	.42	7,400	.0076	1.46	.40	482	2,080	
16	20,900	.22	7,170	.0071	.486	.38	180	2,420	
17	21,600	.081	6,990	.0068	1.05	.41	375	27,300	
18	21,900	.037	6,820	.0067	.519	.34	228	62,400	
19*	24,500	.55	8,490	.0068	6.27	.50	1,850	5,120	
20*	24,700	.47	8,520	.0069	4.56	.50	1,320	4,760	
21*	26,300	.55	8,880	.0066	8.02	.48	2,540	6,930	
22*	30,960	.52	10,500	.0067	32.6	.40	12,100	37,400	
23*	31,040	.56	10,900	.0067	52.2	.48	16,200	44,000	1P28 data
24*	29,420	.54	9,940	.0067	63.6	.53	17,900	51,200	
25*	30,260	.14	9,780	.0066	23.6	.50	7,150	215,000	
26*	30,540	.033	9,320	.0062	4.91	.50	1,580	530,000	
27	18,760	1.13	7,180	.0064	6.32	.70	1,410	1,140	
28	19,000	1.14	7,240	.0064	6.32	.70	1,410	1,130	

*Shot made into advancing air stream; all other shots made into still air.

[redacted]

[redacted]

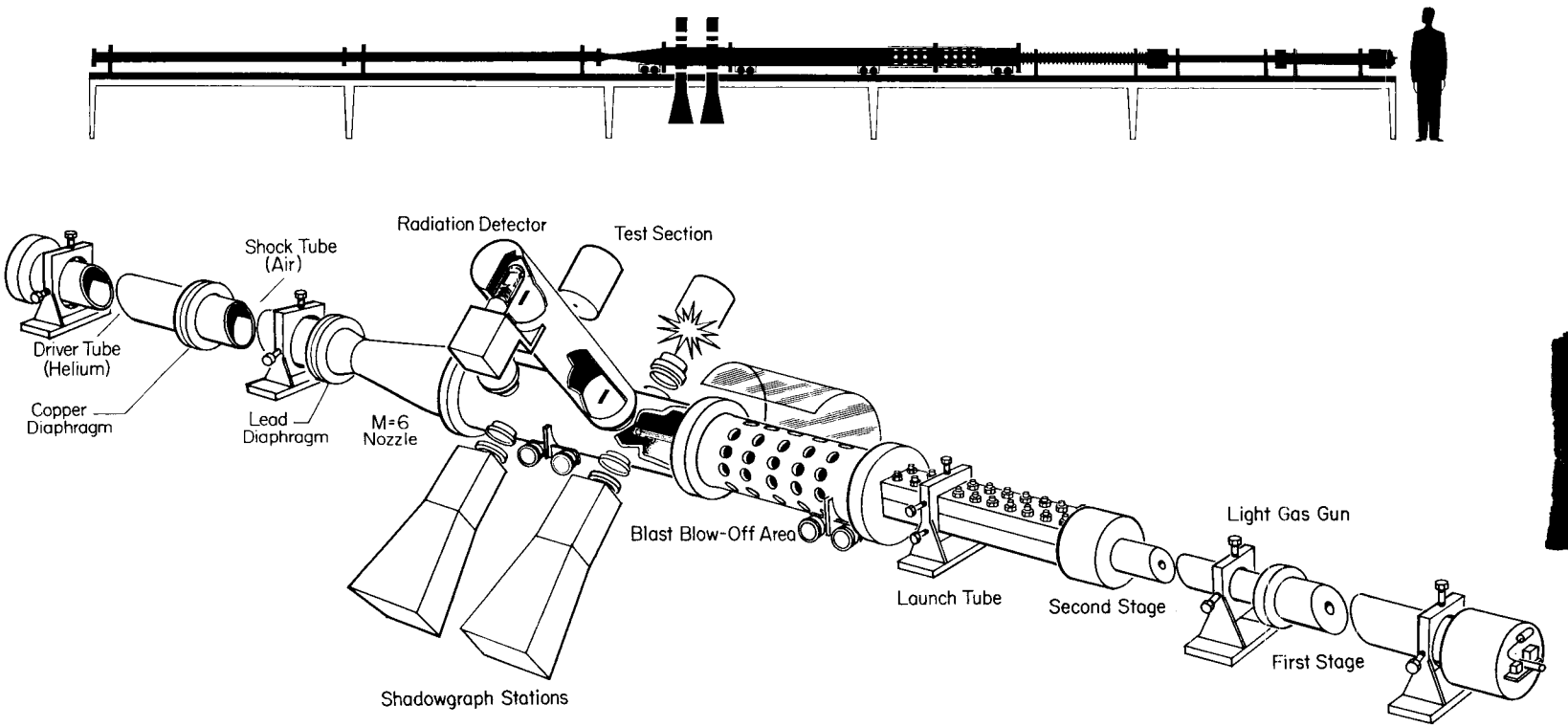

Figure 1.- Schematic drawing of pilot hypersonic free-flight facility.

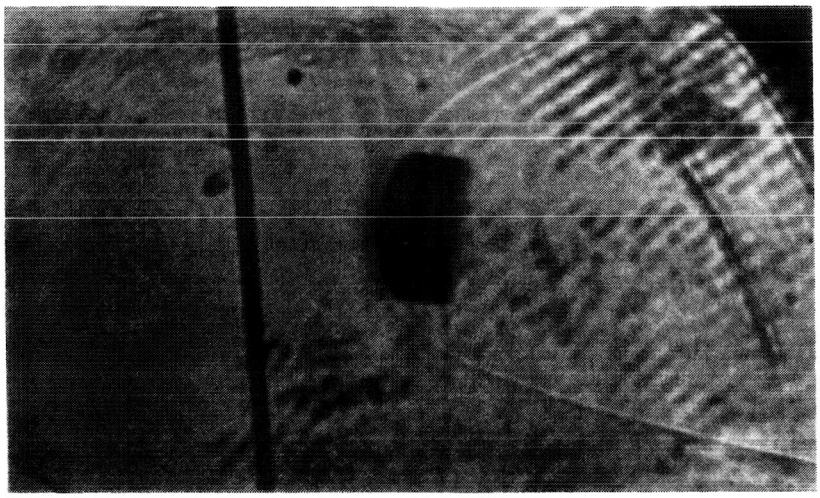

Figure 2.- Typical shadowgraph of model.

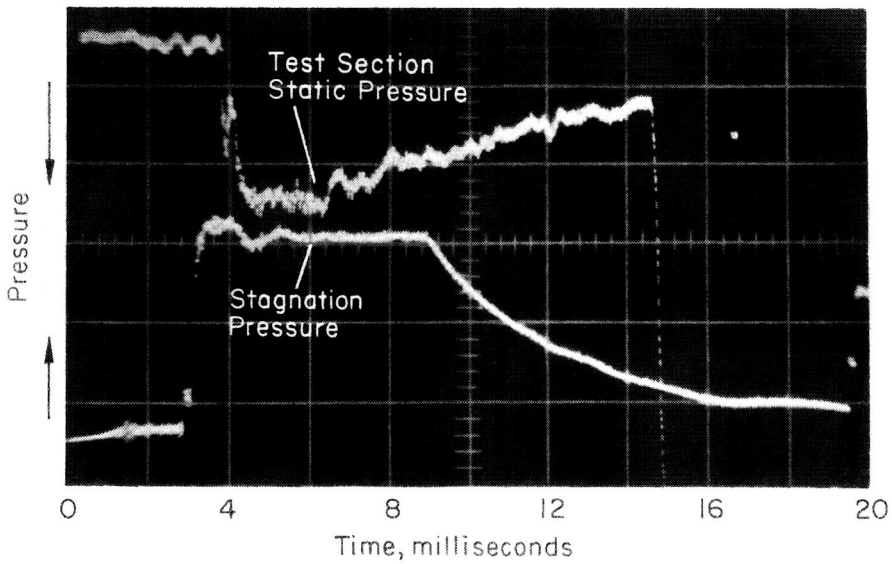

Figure 3.- Typical oscilloscope record of pressures from shock-tube-driven wind tunnel.

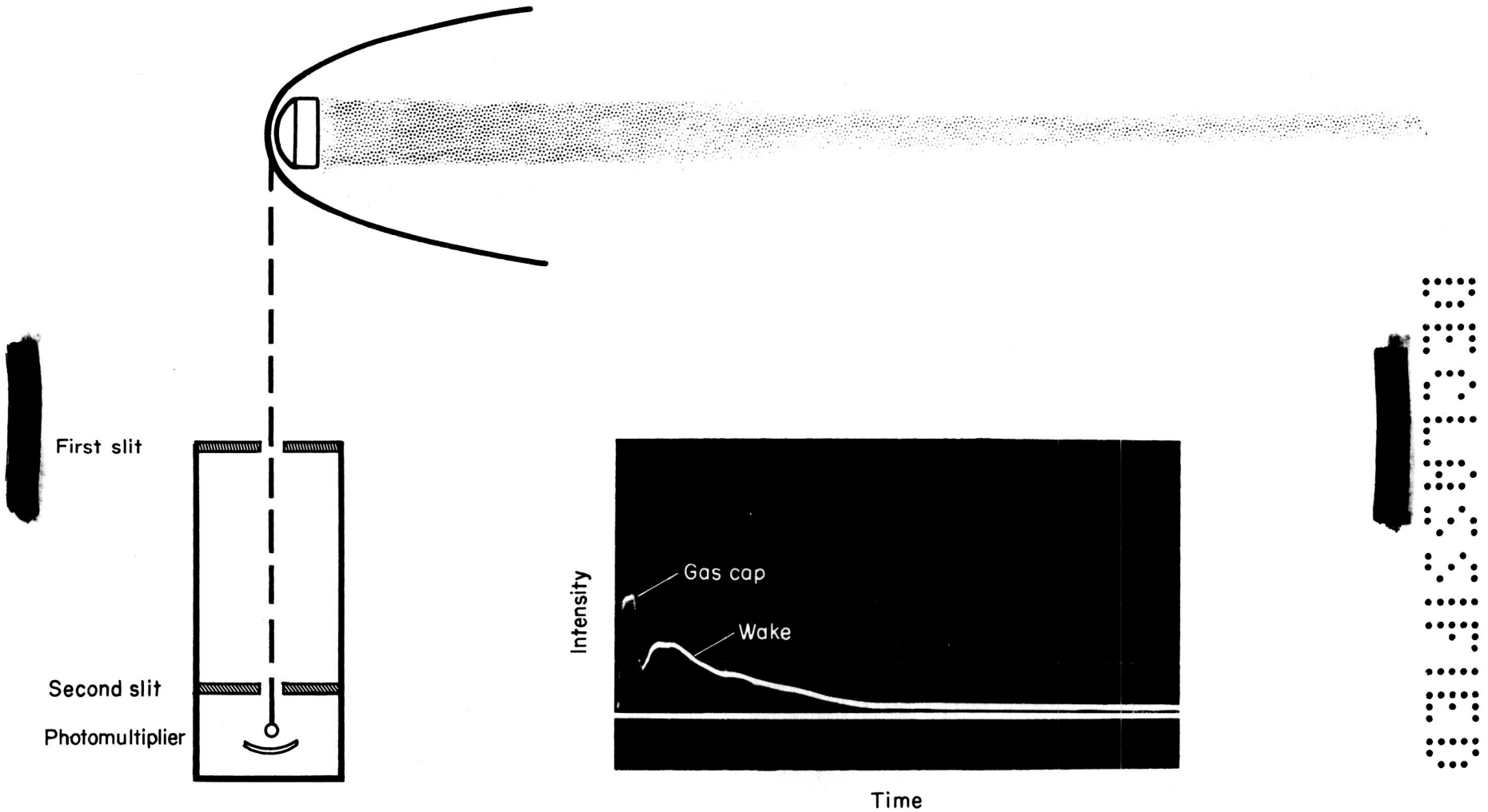

Figure 4.- Experimental setup and typical radiation trace.

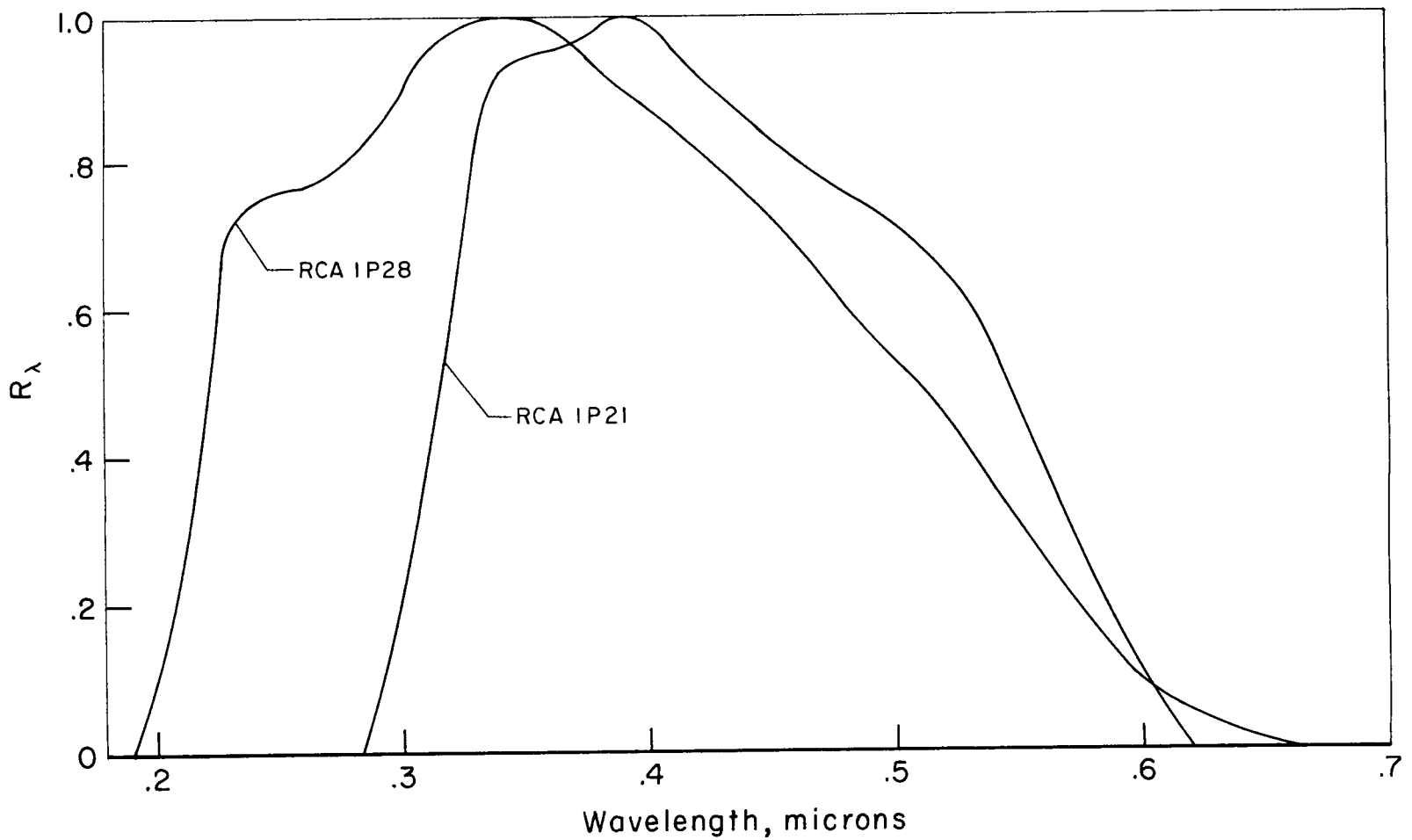

Figure 5.- Response of photomultiplier tubes used during investigation.

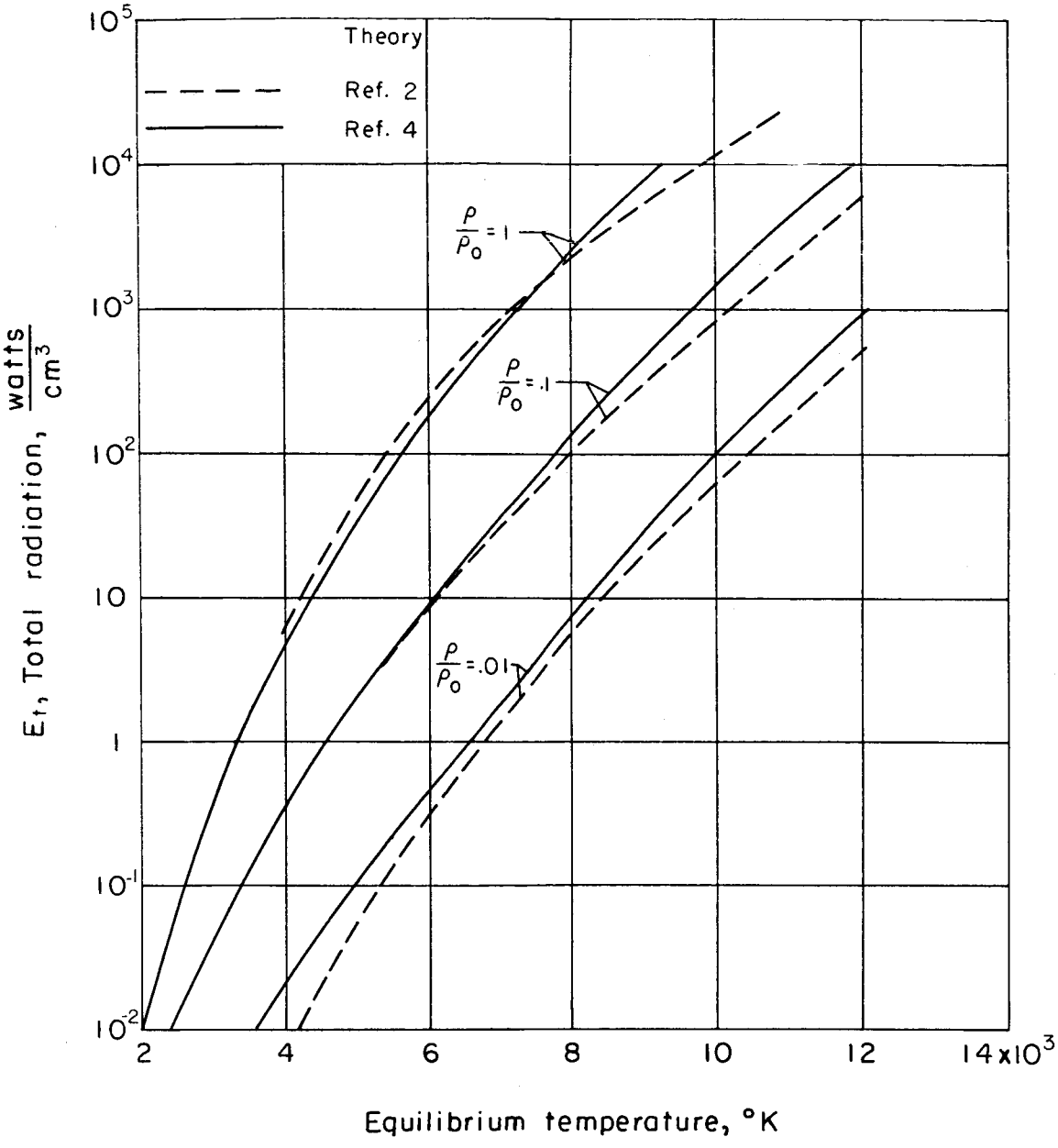

Figure 6.- Comparison of theories for equilibrium radiation from air.

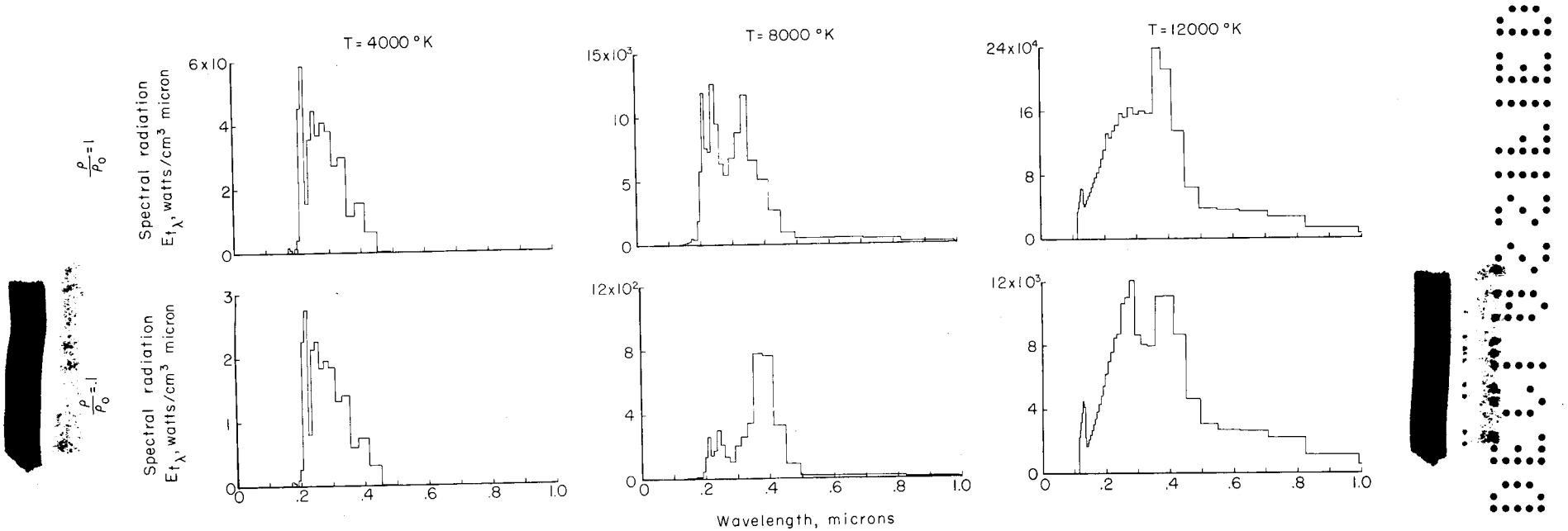

Figure 7.- Theoretical spectral radiation distributions for air in equilibrium from reference 2.

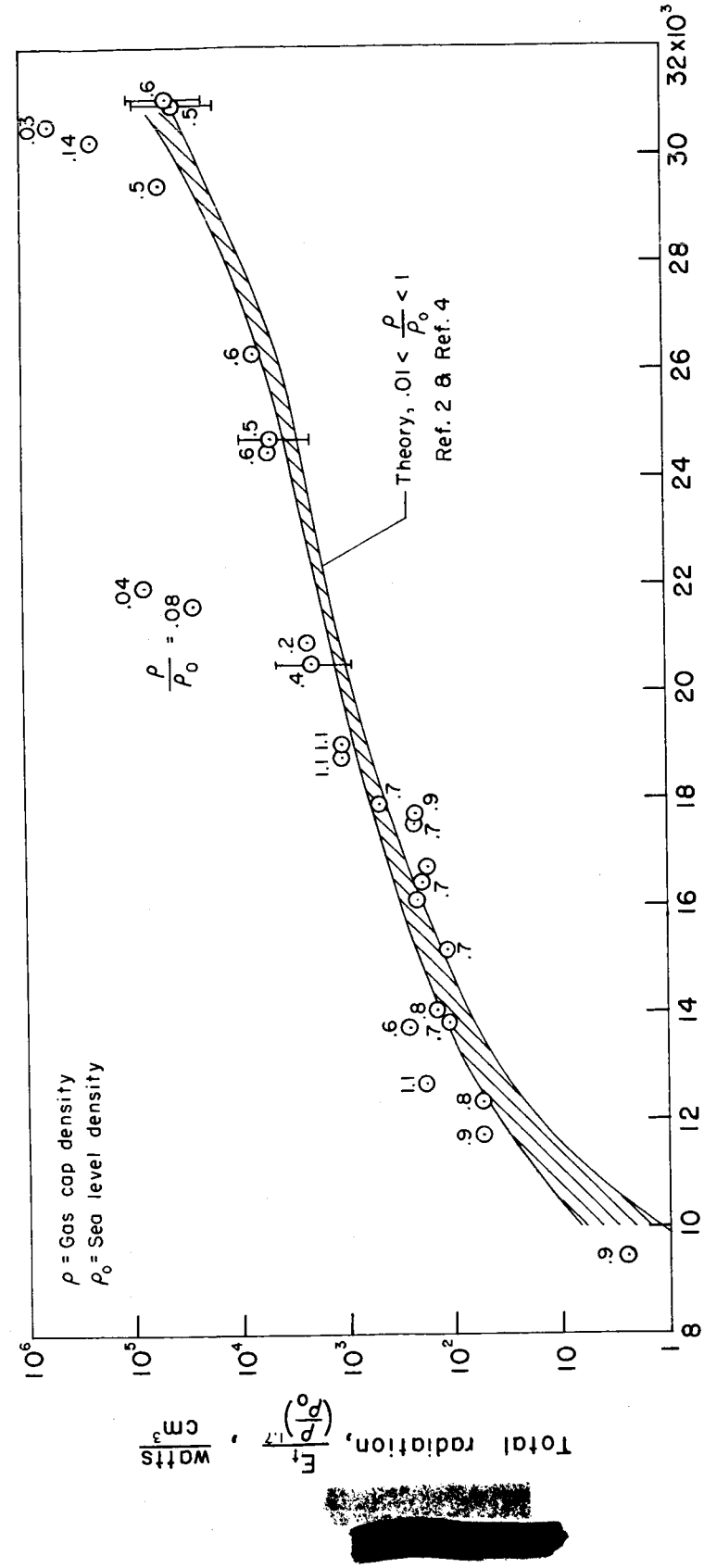

Figure 8.- Comparison of experimental gas-cap radiation with equilibrium radiation theory.

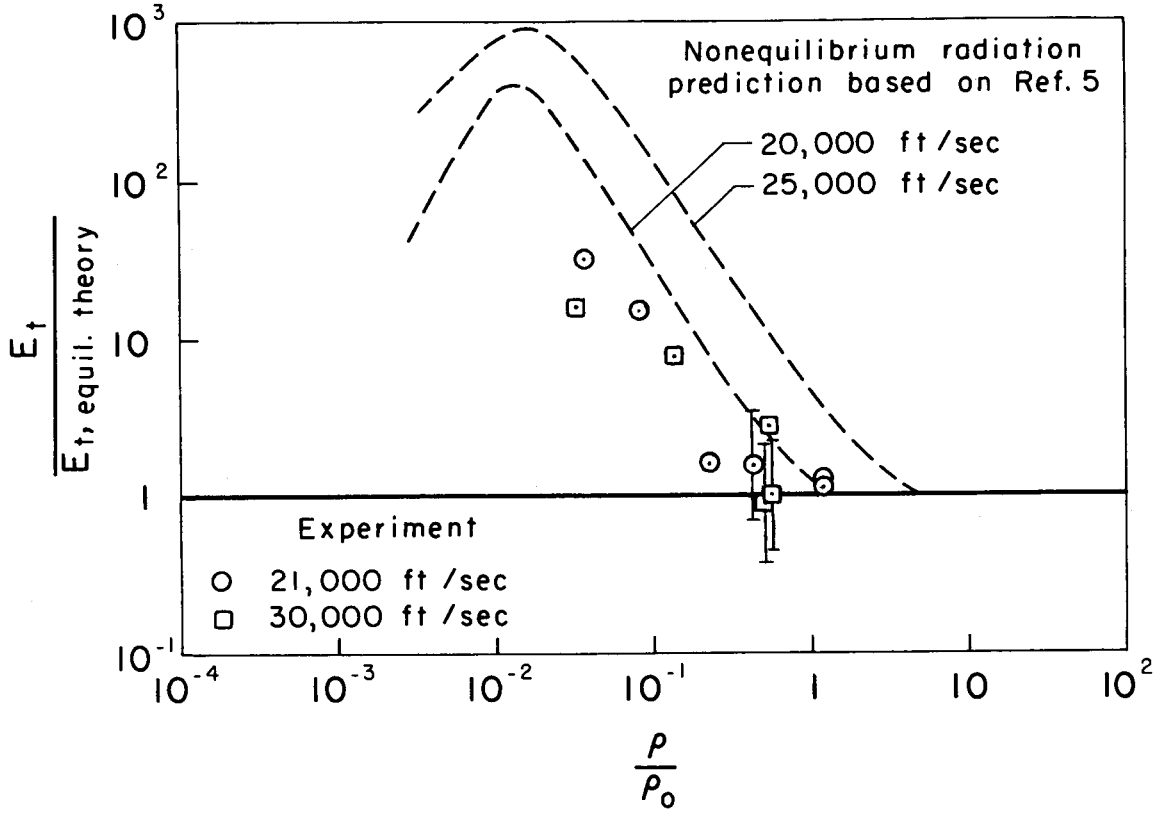

Figure 9.- Comparison of nonequilibrium radiation predictions from reference 5 with experiment for a vehicle with a nose radius of 0.2 inch.

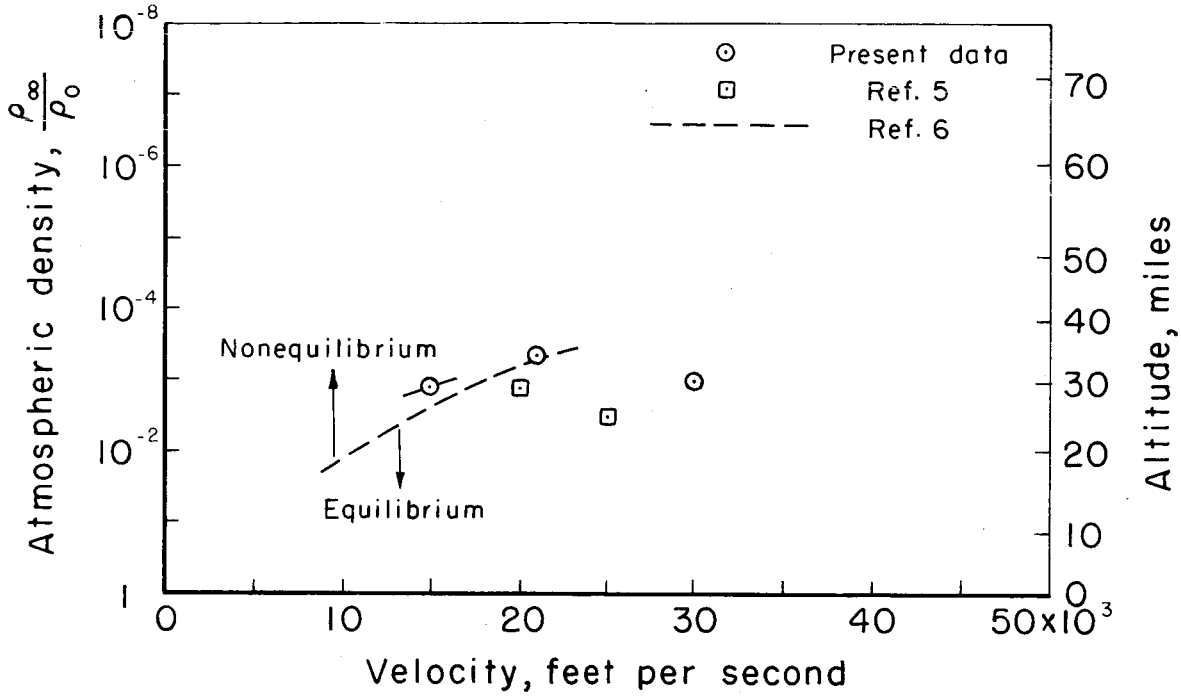

Figure 10.- Predictions for the onset of nonequilibrium radiation for a vehicle with a nose radius of 1 foot.